

A Ground Track Control Algorithm for the Topographic Mapping Laser Altimeter (TMLA)*

V. Blaes, R. McIntosh, and L. Roszman
 Computer Sciences Corporation (CSC)

J. Cooley
 Goddard Space Flight Center (GSFC)

5/2/93
 N93-24707
 15
 P. 13

Abstract

The Topographic Mapping Laser Altimeter (TMLA) will measure the surface elevation of the Earth's landmass and ice sheets to 10-cm precision. With the spacecraft flying in a polar Sun-synchronous orbit in the altitude range of 350 to 400 km, the laser altimeter will illuminate three 100-m diameter circular spots on the ground and scan rapidly in the cross track direction, producing a swath width of 6 km. The objective is to cover the entire Earth gradually, overlapping slightly between adjacent swaths. Providing complete Earth coverage requires precise ground track control, necessitating frequent maneuvers to counteract the effects of atmospheric drag. Therefore, the spacecraft will carry a propulsion system with small thrusters for this purpose.

This paper presents the results of an analysis of an algorithm that will provide autonomous onboard orbit control using orbits determined with Global Positioning System (GPS) data. The algorithm uses the GPS data to (1) compute the ground track error relative to a fixed longitude grid and (2) determine the altitude adjustment required to correct the longitude error. A program was written on a personal computer (PC) to test the concept for numerous altitudes and values of solar flux using a simplified orbit model including only the J_2 zonal harmonic and simple orbit decay computations. The algorithm was then implemented in a precision orbit propagation program having a full range of perturbations. The analysis showed that, even with all perturbations (including actual time histories of solar flux variation), the algorithm could effectively control the spacecraft ground track and yield more than 99 percent Earth coverage in the time required to complete one coverage cycle on the fixed longitude grid (220 to 230 days depending on altitude and overlap allowance).

1. INTRODUCTION

The objective of the Topographic Mapping Laser Altimeter (TMLA) mission will be to measure the surface elevation of the Earth's landmass and landmass ice sheets to submeter (10 cm) precision. The TMLA spacecraft will be launched into orbit by an enhanced Scout or Pegasus booster on or about 1 June 1999. The anticipated mission lifetime will be 3 years with a 30 percent duty cycle.

The spacecraft will fly in a low, Sun-synchronous Earth orbit, with 6 a.m. ascending node nodal crossings. A laser altimeter illuminates three 100-m diameter circular spots on the ground, which are rapidly scanned in the across-track direction. The combined swath width scanned by the lasers is 6 km. Figure 1 illustrates the laser ground scanning geometry. A sweep rate of 70 scans per second produces a 100-m along-track interval between successive scans. The satellite incorporates a hydrazine/electric-arc-jet thruster with a thrust of 0.01 lbs. The specific impulse of the thruster is

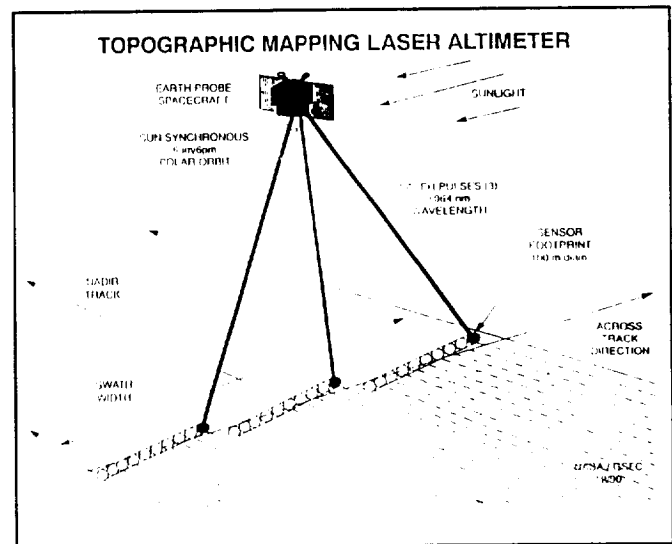


Figure 1. Topographic Mapping Laser Altimeter

* This work was supported by the National Aeronautics and Space Administration (NASA)/Goddard Space Flight Center (GSFC), Greenbelt, Maryland, Contract NAS 5-31500.

in the range of 600 to 800 sec when electric power is supplied to the thruster or 250 to 300 sec without electric power. Ground track positions for the science measurements will be determined from Global Positioning System (GPS) data.

This paper introduces a concept for autonomous ground track control using GPS data as the primary data type. The onboard computer (OBC) determines longitude position errors at the ascending nodes and commands altitude-raising maneuvers to correct those errors. The following steps were carried out in the development of the ground track control algorithm:

- For a range of orbit skip cycles, the altitudes required for efficient ground coverage (i.e., sensor ground swaths with specified, small overlaps) were determined for a range of altitudes between 300 and 400 km using a 6-km ground swath width.
- An algorithm for autonomous orbit control was developed on a personal computer (PC) using a simplified analytical two-body model.
- Performance of the orbit control algorithm was determined with a realistic Earth gravity field, third body perturbations, and solar flux variations, using the Goddard Mission Analysis System (GMAS).

It was concluded that the ground track control algorithm developed could meet the coverage objectives in a 3-year mission.

2. ALTITUDES FOR REPEATING GROUND TRACKS

Complete Earth coverage requires choosing an altitude that results in sufficient overlap of adjacent swaths to cover the dispersions in ground track position attributable to orbit control inaccuracies and all other orbit perturbations. Frequent altitude-raising maneuvers are required to maintain the desired ground track overlap and avoid gaps in coverage. The number of orbits between adjacent ground tracks (the repeat cycle) and the minimum number of orbits necessary for complete Earth coverage are functions of the nominal orbit altitude, the swath width, and swath overlap, assuming no orbit perturbations.

The geometry associated with ground track spacing and swath coverage is illustrated in Figure 2. The longitude interval, DL , between successive ascending nodes for repeat cycle, R , and ground track spacing, S , for an eastward-advancing ground track is

$$\text{Mod}(R \times |DL|)_{360} = 360 - \frac{S}{R_e} \times \frac{\pi}{180}, \text{ deg} \quad (1)$$

and for a westward-advancing ground track by

$$\text{Mod}(R \times |DL|)_{360} = \frac{S}{R_e} \times \frac{\pi}{180}, \text{ deg} \quad (1a)$$

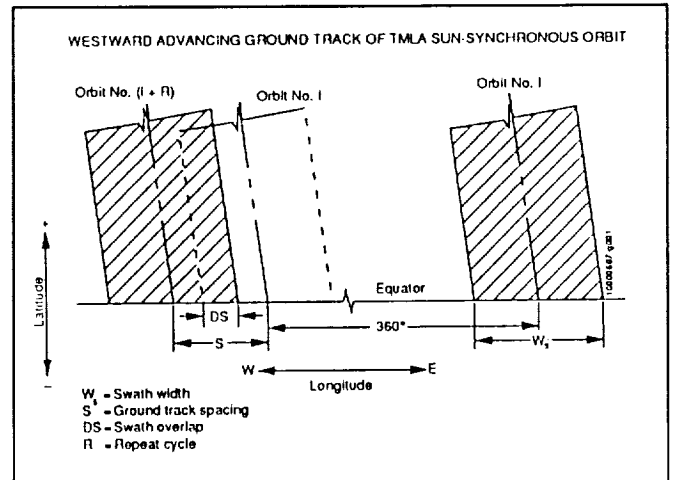


Figure 2. Westward-Advancing Ground Track of TMLA Sun-Synchronous Orbit

For a Sun-synchronous orbit,

$$DL = \left[\omega_e + \frac{360}{T_y} \right] \times 2\pi \left[\frac{a^3}{\mu} \right]^{\frac{1}{2}}, \text{ deg}, \quad (2)$$

- where ω_e = rotational rate of the Earth (deg/sec)
 T_y = length of a sidereal year in seconds
 a = semimajor axis
 μ (km^3/sec^2) = Earth's gravitational attraction

The semimajor axis is the sum of the spherical Earth radius, R_e , and height, H , above the ground:

$$a = R_e + H = 6378.14 + H, \text{ km} \quad (3)$$

Because the equator is traversed twice in every orbit, the minimum number of orbits needed for complete Earth coverage is

$$N_{\min} = \frac{\pi R_e}{(W_s - DS)}, \text{ orbits} \quad (4)$$

where W_s is the swath width, and DS is the swath overlap distance. The nominal spacing, S , between ground tracks at the equator is $S = W_s - DS$. Complete Earth coverage for a given repeat cycle and nominal altitude is seldom obtained in exactly N_{\min} orbits.

The repeat cycle is efficient if the number of orbits needed for complete Earth coverage is not significantly greater than N_{min} . Equations 1 and 2 were solved for values of S equal to 5.6 and 5.8 km (overlap of 0.4 km and 0.2 km) in a range of R between 50 and 600 and a range of altitudes between 300 and 400 km. Altitudes with a potential for producing a high percentage total coverage in N_{min} orbits were selected to evaluate the ground track control algorithm.

3. GROUND TRACK CONTROL ALGORITHM

At every ascending node, the OBC determines whether an orbit maneuver is needed to correct a ground track error. The longitude at the ascending node is determined from GPS data. The longitude error is the difference between the observed longitude and a nominal longitude. The sign of the error determines whether the spacecraft is too high or too low. If the longitude error is positive, the altitude must be raised, and a Hohmann orbit-raising maneuver is used; otherwise, no maneuver is performed. The first burn of the Hohmann orbit maneuver is performed at the ascending node; the second burn is performed half an orbit later. The OBC determines when an ascending node is reached, then computes a longitude error, determines the necessary thruster burn times if a maneuver is required, and issues commands to start and stop the burns. The orbit control algorithm has two control modes.

Control Mode 1

Control Mode 1 uses a relative longitude error, defined as the difference between two longitude differences; one is the difference between estimated longitudes at two successive ascending nodes, the other is an uplinked reference delta longitude (the difference between longitudes of successive ascending nodes of a reference orbit). In this control mode, the spacecraft altitude is caused to move toward the nominal altitude. This mode is used only after orbit injection, or after a command to change the nominal altitude is uplinked from the ground.

Control Mode 2

Control Mode 2 is based on an absolute longitude error. The absolute error is the difference between the estimated longitude and a longitude obtained from a fixed-longitude grid. The first longitude of the fixed-longitude grid is created by setting it equal to the estimated longitude the first time the sign of the relative longitude error in Mode 1 changes, which occurs when the nominal altitude is reached. Thereafter, a new reference longitude is computed at every node by adding the uplinked reference delta longitude to the longitude at the previous nodal crossing. The reference delta longitude is changed only if it becomes necessary to change the reference altitude. Ground support for satellite naviga-

tion consists entirely of uplinking a reference delta longitude, when needed, and uplinking the measured solar flux at regular intervals.

The Control Equation

The altitude correction required to cancel a ground track error consists of two parts. One part results from a longitude error at the ascending node, the other part results from the rate of change of the longitude error. Each part is the product of a gain constant and a corresponding error, divided by the sensitivity of the delta longitude between successive ascending nodes to a change in the semimajor axis. The resulting semimajor axis correction is as follows:

$$\Delta a = \frac{k_d \Delta \lambda_i + k_r \frac{d}{dt} (\Delta \lambda_i)}{\frac{d\lambda_i}{da}} \quad (5)$$

where k_d is the dimensionless displacement gain constant, and k_r is the dimensionless rate gain constant.

$$\frac{d\lambda_i}{da} = \frac{180}{\pi} (\omega_e - \dot{\Omega}) P, \text{ deg/km} \quad (6)$$

where P is the orbital period, ω_e is the Earth's rotation rate, and $\dot{\Omega}$ is the node rate.

The rate error term damps longitude error oscillations. The nodal regression rate, $\dot{\Omega}$, is a function of the semimajor axis, a , eccentricity, e , and orbit inclination, i . The following relation for $\dot{\Omega}$ from Reference 1 is accurate to first order in J_2 .

$$\begin{aligned} \dot{\Omega} &\approx -\frac{3}{2} J_2 \sqrt{\mu} R_e^2 a^{-7} (1 - e^2)^{-2} \cos(i) \\ &= \frac{-2.06474 \times 10^{14} \times \cos(i)}{a^7 \times (1 - e^2)^2 \times 86164.09} \end{aligned} \quad (7)$$

The semimajor axis, a , in Equation 7 is assumed to be constant, and eccentricity is assumed to be zero.

In the simulation, the estimated longitude at the node is assumed to have a standard deviation of 30 m, with a Gaussian distribution and zero mean.

4. PC SIMULATION OF AUTONOMOUS ORBIT CONTROL

The orbit control algorithm was tested in a PC program to investigate the feasibility of the concept. Several simplifying assumptions were made:

- Two-body analytic circular orbits, with J_2 only.
- The semimajor axis reduction per orbit due to atmospheric drag is approximated from energy considerations; hence, integration of the equations of motion is not necessary.
- Instantaneous altitude corrections are made at the ascending node.
- An exponential density is fitted to the Harris-Priester (H-P) atmospheric density model between 300 and 400 km altitude. Density is modeled empirically as a function of solar flux and adjusted for the effects of the atmospheric bulge.

Altitude Loss Per Orbit

A calculation is made at every ascending node to determine the altitude loss in the preceding orbit. The altitude loss is obtained by equating the energy loss in one orbit to the work done by the drag force on the spacecraft. The work done by the drag force, D , is

$$W = 2\pi a D = \pi a \rho C_d A V^2, N \cdot m \quad (8)$$

where A = reference area (m^2)
 a = semimajor axis (m)
 ρ = atmospheric density
 C_d = drag coefficient
 V = velocity

The total energy loss per orbit (potential plus kinetic) is

$$E = -\frac{1}{2} \mu m \left[\frac{1}{a_i} - \frac{1}{a_f} \right], N \cdot m \quad (9)$$

where a_i and a_f are initial and final values of semimajor axis, and m is the spacecraft mass. Because

$$a_{avg}^2 \approx a_i a_f \quad (10)$$

the change in the semimajor axis, $\Delta a = (a_i - a_f)$, from Equations 8 and 9 becomes equal to

$$\Delta a = -2\pi \rho \frac{C_d A}{m} a_{avg}^2 \quad (11)$$

The Atmospheric Density Approximation

The H-P density between altitudes of 300 and 400 km was approximated at solar flux levels of 80 and 240 by exponential functions fitted to an orbital density intermediate between the minimum and maximum density values in the H-P density model. The intermediate value was equal to the H-P minimum, plus 0.2 times the difference between the

H-P maximum and minimum densities. It approximates the effects of an atmospheric bulge on the density for a Sun-synchronous (0600 hrs ascending node) TMLA orbit. The atmospheric density equations for the 300 to 400 km altitude range are as follows:

$$\text{For solar flux level of 80,} \quad (12)$$

$$\rho = 5.761091 \times \text{Exp}(-0.0216952 H), \text{ kg/km}^3$$

$$\text{For solar flux level of 240,} \quad (13)$$

$$\rho = 4.142531 \times \text{Exp}(-0.01566959 H), \text{ kg/km}^3$$

The exponential density functions are compared with H-P data at 20 km intervals between 300 and 400 km altitude in Figure 3. The solar flux is measured at the 10.7 cm wave length ($F_{10.7}$) and is in units of 10^{-22} Watts/ m^2 /Hertz.

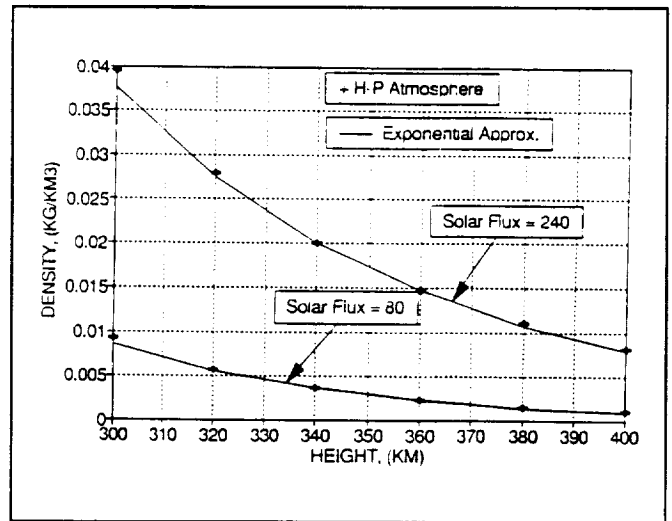


Figure 3. Atmospheric Density Functions Compared With H-P Data

Optimized Control Gain Constants

Values of k_d and k_r that minimize the dispersion of longitude error were determined experimentally from runs made with constant flux values of 80 and 240 (Equations 12 and 13). The control gains, formulated as functions of altitude and solar flux, are given in the following equations, which are the default optimum control gains in the PC simulation.

$$k_d = 0.08 + F_{10.7} \quad (14)$$

$$\times (0.0083 - 0.325 \times 10^{-4} H + 3.0 \times 10^{-8} H^2)$$

$$k_r = 0.0035 \quad (15)$$

In Figure 4, k_d is presented as a function of altitude and solar flux.

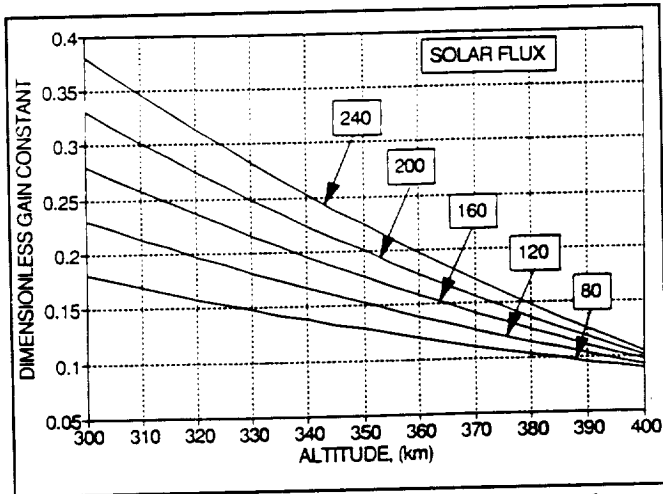


Figure 4. Displacement Gain as a Function of Altitude and Solar Flux

PC Simulation Numerical Results

A sequence of runs with optimum control gains was made to determine the effects of ground track spacing, altitude, solar flux, and position measurement accuracy on the standard deviation of the controlled position error and the total delta-V for N_{min} orbits. The solar flux was either held constant at 80 or 240, or else actual past daily values of $F_{10.7}$ from a flux file were used (covering a period of time in which the flux levels approximated the levels predicted by Schatten (Reference 2) after the TMLA epoch).

Constant Solar Flux

Numerical results are presented in Table 1 for a nominal ground track spacing of 5.8 km; altitudes of 300, 350, and 400 km; constant solar flux values of 80 and 240; and measurement noise standard deviations of 0 and 30 m. The standard deviation of the longitude distance error for perfect position measurements is between 3 and 7 meters, due largely to a transient at the start of the runs. For a 30 m measurement noise, the standard deviation of the distance error is 37 to 39 m for both low and high flux values (i.e., up to 30 percent larger than the measurement noise). An

Table 1. Orbit Control Performance From PC Simulation Based on Constant Solar Flux

NOMINAL GROUND TRACK SPACING = 5.8 KM
3455 ORBITS; $I_{sp} = 275$ LBM-SEC/LBM

Nom Alt (km)	Flux	Meas. Noise (m)	Distance Error (m)			Altitude (km)	v_{prop} (ft/s)	v_{NB}^* (m/s)	Delta V (m/s)	Burn Per Maneuv. (sec)	
			Std. Dev.	Min	Max						
300	240	0	-3	146	5	299.686	300.090	47.30	3455	264.11	188.3
300	80	0	-81	193	6	299.827	300.018	18.94	3455	102.70	75.4
300	240	30	-131	147	37	299.748	300.075	36.57	3455	201.87	145.5
300	80	30	-130	148	37	299.862	300.153	11.38	3455	61.19	45.2
350	240	0	-9	313	6	349.866	350.040	22.82	3455	124.18	90.8
350	80	0	-21	60	3	349.877	349.978	11.90	3455	64.03	47.3
350	240	30	-132	168	38	349.808	350.123	17.94	3455	97.12	71.3
350	80	30	-127	176	39	349.849	350.175	7.37	3455	29.49	29.2
400	240	0	-2	96	6	399.877	399.989	14.41	3455	77.76	57.4
400	80	0	-4	88	7	339.927	400.037	9.96	3455	53.48	39.6
400	240	30	-131	146	37	399.834	400.145	10.45	3455	56.13	41.6
400	80	30	-115	160	38	399.856	400.160	6.06	3455	32.44	24.1

orbit maneuver is required at every ascending node. Total mission delta-V, based on propellant specific impulse (I_{sp}) of 275 seconds, ranges from a low of 32.44 m/s for an altitude of 400 km with a low flux, to a high of 262.11 m/s for an altitude of 300 km with a high flux. Burn times (half of a Hohmann maneuver) for the 0.01 lb thruster ranged between 24.1 and 188.3 sec for the two altitude and flux conditions investigated.

Similar data for a 5.6 km nominal ground track spacing are presented in Table 2. The control error statistics are unaffected by the ground track spacing. However, because

Table 2. Orbit Control Performance From PC Simulation Based on Constant Solar Flux

NOMINAL GROUND TRACK SPACING = 5.6 KM
3579 ORBITS; $I_{sp} = 275$ SEC

Nom Alt (km)	Flux	Meas. Noise (m)	Distance Error (m)			Altitude (km)	v_{prop} (ft/s)	v_{NB}^* (m/s)	Delta V (m/s)	Burn Per Maneuv. (sec)	
			Std. Dev.	Min	Max						
300	240	0	-3	146	5	299.686	300.090	48.92	3578	273.59	187.9
300	80	0	-81	193	6	299.827	300.018	19.61	3579	106.36	75.3
300	240	30	-131	147	37	299.797	300.075	37.83	3579	209.10	145.3
300	80	30	-130	148	37	299.824	300.153	11.75	3579	63.23	45.1
350	240	0	-9	313	6	349.866	350.040	23.62	3579	128.63	90.7
350	80	0	-21	60	3	349.877	349.978	12.32	3579	66.32	47.3
350	240	30	-132	168	38	349.806	350.123	18.55	3579	100.53	71.3
350	80	30	-127	176	39	349.847	350.175	7.61	3579	40.75	29.2
400	240	0	-2	96	6	399.877	399.989	14.92	3579	80.55	57.3
400	80	0	-4	88	7	339.927	400.037	10.31	3579	55.40	39.6
400	240	30	-131	146	37	399.834	400.145	10.84	3579	58.29	41.7
400	80	30	-115	160	38	399.856	400.160	6.30	3579	33.71	24.2

* NB is the number of orbits with orbit-raising maneuvers

more orbits (N_{min}) are necessary to obtain total coverage, the total delta-V is increased by the ratio of $5.8/5.6 = 1.0357$.

The standard deviation of position errors shown in Tables 1 and 2 is a useful measure of the control accuracy obtainable from the algorithm. The standard deviations do not translate directly into a percent coverage; however, when the nominal altitude is properly chosen, smaller position error dispersions correlate with a higher percent coverage for a given swath overlap.

Daily Varying Solar Flux

A daily solar flux variation from observations made during the last solar cycle that approximates the predicted solar flux variation after the TMLA epoch is presented in Figure 5. This flux variation was used to determine the altitude loss per orbit. The same data, delayed one day, were used as the flux input to the control law. This simulated an operational scenario in which the 1-day-old measured solar fluxes would be uplinked daily.

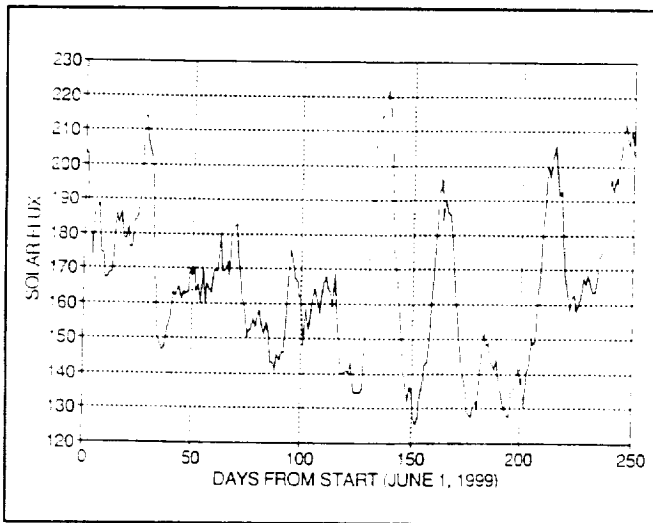


Figure 5. Daily Solar Flux for TMLA Simulation

The performance of the control law with the daily solar flux data is presented in Table 3 for a ground track spacing of 5.8 km and in Table 4 for a ground track spacing of 5.6 km. With no error in orbit determination, the standard deviation of distance error is 1.6 to 4.2 times greater than when solar flux is constant, the error decreasing with an increase of altitude. With a 30 m orbit determination accuracy, the standard deviation of position error is 24 percent greater at an altitude of 300 km than if solar flux were constant, but only 1 percent greater at an altitude of 400 km. For a daily flux variation and a 30 m orbit determination error, the ratios of the standard deviation of longitude error to the nominal overlap (6 km swath minus

Table 3. Orbit Control Performance From PC Simulation Gain Constants Based on 1-Day-Old Solar Flux

NOMINAL GROUND TRACE SPACING = 5.8 KM
3455 ORBITS; $t_{sp} = 275$ SEC

Nom Alt (km)	Meas. Noise (m)	Distance Error (m)			Altitude (km)		W_{prop} (lbs)	NB*	Delta V (m/s)	Burn Per Maneuv. (sec)
		Min	Max	Std Dev	Min	Max				
300	0	-107	312	21	299.649	300.056	33.46	3455	184.08	133.1
300	30	-174	198	48	299.646	300.151	34.68	3455	191.06	138.0
350	0	-95	236	14	349.741	350.027	18.26	3455	98.90	72.7
350	30	-157	156	42	349.744	350.163	20.31	3455	110.24	80.8
400	0	-33	251	11	399.852	399.969	14.11	3455	76.11	56.2
400	30	-134	151	39	399.780	400.150	15.97	3455	86.31	63.6

Table 4. Orbit Control Performance From PC Simulation Gain Constants Based on 1-Day-Old Solar Flux

NOMINAL GROUND TRACE SPACING = 5.6 KM
3579 ORBITS; $t_{sp} = 275$ SEC

Nom Alt (km)	Meas. Noise (m)	Distance Error (m)			Altitude (km)		W_{prop} (lbs)	NB*	Delta V (m/s)	Burn Per Maneuv. (sec)
		Min	Max	Std Dev	Min	Max				
300	0	-107	312	21	299.649	300.056	34.63	3579	190.79	137.8
300	30	-174	198	47	299.646	300.151	35.88	3579	197.93	137.9
350	0	-95	236	13	349.741	350.027	18.94	3579	102.63	72.7
350	30	-157	156	42	349.744	350.163	21.04	3579	114.3	80.8
400	0	-33	251	11	399.852	399.969	14.63	3579	78.97	56.2
400	30	-134	151	39	399.780	400.150	16.55	3579	89.46	63.6

* NB is the number of orbits with orbit-raising maneuvers

the ground track spacing) and the maximum longitude error to the overlap are summarized below:

Altitude	Std Dev/Overlap	Max Error/Overlap
300	0.12	0.50
350	0.11	0.39
400	0.10	0.38

With careful selection of the nominal altitude, the percent coverage for ground track spacing of 5.6 and 5.8 km at low or high altitude in the 300 to 400 km range is between 98.35 and 99.98 percent in N_{min} orbits. On the basis of these results, it was concluded that the performance of the TMLA ground track control algorithm merited further analysis, including the effects of orbit perturbations from higher order gravitational potential model terms and third-body effects of the Sun and Moon. Additional analyses were, therefore, performed using the Goddard Mission

Analysis System (GMAS) program. Those analyses are described in the sections that follow.

5. GMAS SIMULATION OF AUTONOMOUS ORBIT CONTROL

The orbit control algorithm detailed in the previous sections was implemented in a special module for use with the GMAS Cowell orbit propagator. This propagator can include perturbations resulting from drag, the geopotential field, and solar and lunar gravitational effects, as desired. The program stops at each ascending node and checks the longitude error from the reference (the error includes simulated measurement noise).

If the error is positive (the altitude is below nominal), the required Hohmann transfer delta-V is computed. Half the delta-V is applied as an impulse at the current nodal crossing, and the remainder is applied at the next descending node. The longitudes at all ascending and descending nodes are recorded for later sorting and generating statistics. Ground track error at each ascending node is also output.

The procedure followed is first to choose a case from the PC simulation that gives good coverage, input the nominal longitude separation between successive nodal crossings (*DLONG*), and iterate on the initial osculating semimajor axis until the longitude separation matches *DLONG*. The GMAS implementation uses only Control Mode 2 (see Section 3), so the simulator must start at the correct altitude. A long run is then made and gains are adjusted in an attempt to improve the resulting coverage.

Computation of statistics involves sorting the crossings in ascending order of longitude, computing the spacing between adjacent longitudes, and summing all the gaps and overlaps. The number of crossings (ascending and descending) used to generate statistics is the theoretical minimum needed to give total coverage. This number is 6910 for a grid with 5.8 km spacing and 7157 for a spacing of 5.6 km. The swath width used in this analysis is 6 km.

Simulations were performed with J_2 only, an 8 by 8 geopotential, constant solar flux, a smoothly varying flux, and daily flux variations for both 5.8 and 5.6 km spacings. Initial runs were made with constant gains in the control law. After the algorithm was verified, the computations for gain as a function of flux described in Section 4 were implemented and runs were made using daily flux variations with a 1-day delay. The results of each are discussed in the following sections.

Initial GMAS Tests

The initial runs were made with J_2 only to simplify the modeling and ensure the algorithm was working properly. The spacecraft was assumed to have a mass of 230 kg, area of 1 m², and coefficient of drag equal to 2.2. The epoch for

all runs is June 1, 1999. Densities were computed with the H-P atmosphere model.

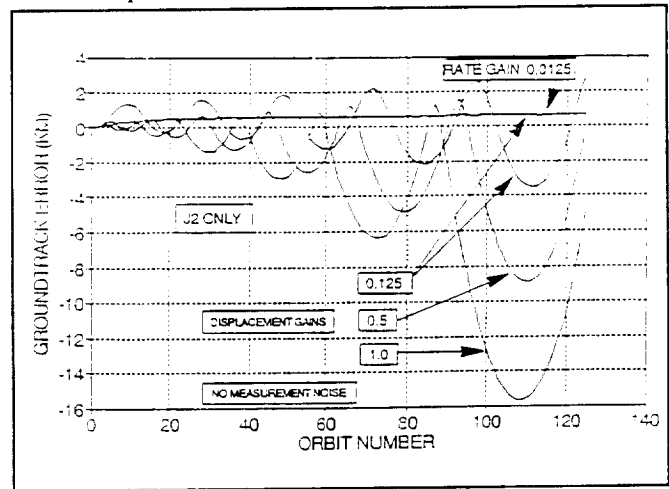


Figure 6. Effect of Various Gain Settings on Ground Track Error

Figure 6 shows the evolution of ground track error for 125 orbits using different gain values. The three curves that show a large buildup in fluctuations did not have a rate gain applied; while the nearly horizontal line from the fourth case used a rate gain of 0.0125. This plot clearly shows the need for using both rate and displacement gains and for choosing good values.

Figure 7 shows the effects of added measurement noise. The noise used in all GMAS simulations assumes a Gaussian distribution with a standard deviation of 30 m, as in the PC simulations. The plot shows ground track error for two sets of displacement gain (DG) and rate gain (RG). The smooth

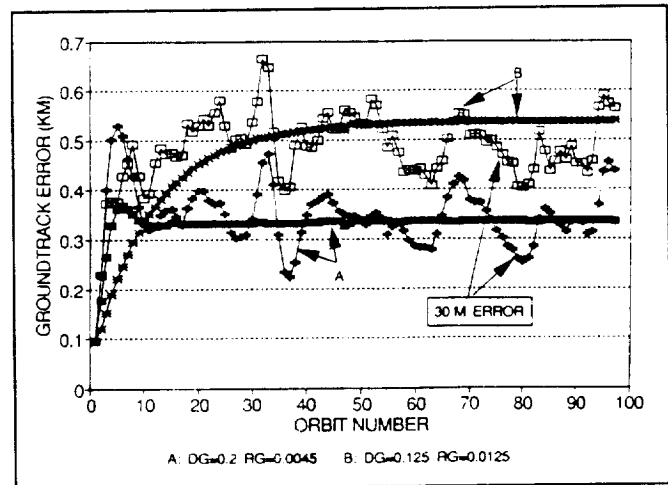


Figure 7. TMLA Ground Track Error J_2 (With and Without 30 M Orbit Error)

curves represent J_2 only with no noise; while the fluctuating ground track error shows the effect of the added noise.

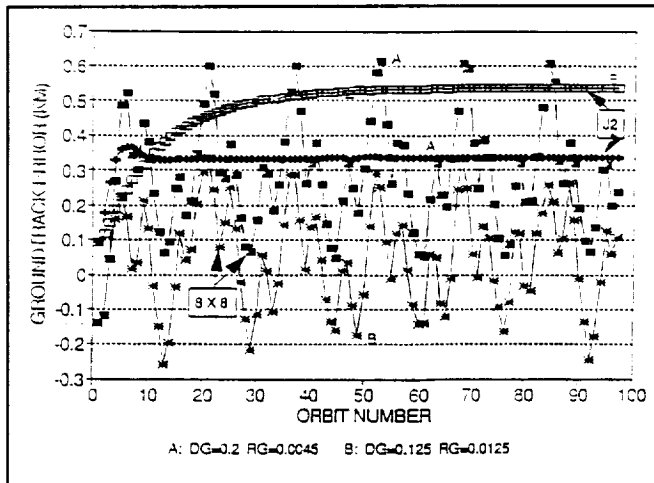


Figure 8. TMLA Ground Track Error J_2 , 8x8, Different Gains

Figure 8 compares the difference between using J_2 only or a more realistic 8 by 8 geopotential model (noise not included). The 8 by 8 model causes the ground track to vary over a range of between 0.5 and 0.6 km.

Figure 9 shows the response of the algorithm to values of solar flux and gains. These runs were made with J_2 only and no noise. The top curve, A, shows the ground track error history for 4000 orbits (8000 nodal crossings) with a slowly increasing flux that follows the Schatten +2 sigma prediction. The predicted flux values for 1 year are as follows:

Date	Flux
Jun 1, 1999	195
Jul 1, 1999	201
Aug 1, 1999	207
Sep 1, 1999	213
Oct 1, 1999	218
Nov 1, 1999	223
Dec 1, 1999	228
Jan 1, 1999	232
Feb 1, 2000	236
Mar 1, 2000	239
Apr 1, 2000	242
May 1, 2000	244
Jun 1, 2000	246

Curve B results from a constant flux of 200. Both A and B use constant gains. The bottom curve, C, shows the error resulting from a flux that varies daily (see Figure 5) and gains that are computed daily from the observed flux. There is a 1-day delay between the observed flux value and the use of that value in the control computations. Coverage statistics were generated for these three cases and are as follows:

Case	Percent Coverage at Equator
A	99.972
B	99.975
C	99.965

Using J_2 only, no orbit error, and a constant flux yields the best total coverage that the algorithm can produce. Adding orbit error, the geopotential, and flux variations for more realistic modeling will always yield less coverage. However, the total coverage can still be above 99 percent, as will be shown later. A coverage of 99.975 percent means that a total of only 10 km (out of 40,075) remains uncovered at the equator.

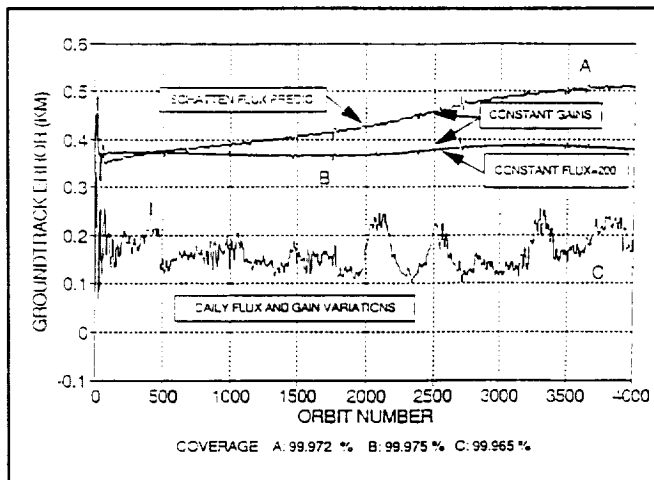


Figure 9. TMLA Ground Track Error J_2 Only, No Noise

GMAS Simulations With All Perturbations

Simulations were run for several different altitudes with grid spacings of both 5.8 and 5.6 km. The spacing is controlled by using the correct semimajor axis in combination with the appropriate value of DLONG for each case. DLONG is the separation in deg between successive equator crossings (one orbit apart) and is a precise number that is determined by the PC program. Using an incorrect value for DLONG results in greatly reduced total coverage. Runs were made first with constant gains and the Schatten flux predictions and then with daily varying flux and gains. The results of each are discussed below.

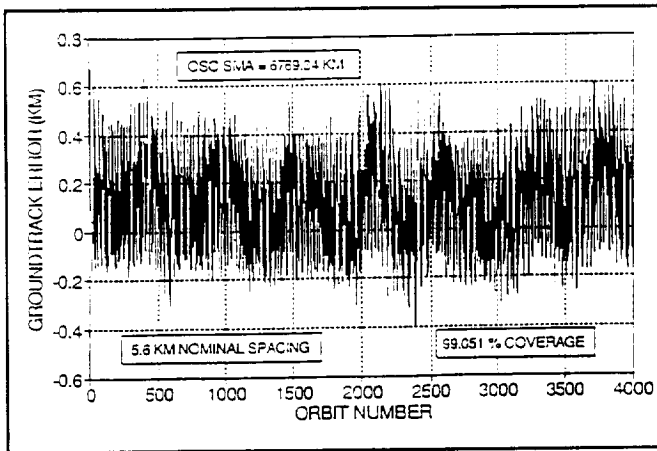


Figure 10. TMLA Ground Track Error Daily Flux Variations (1-Day Delay)

Sample Results With Daily Flux Variations. Figure 10 shows ground track error versus time for a case when the initial osculating semimajor axis is 6769.34 km (391 km altitude at the initial ascending node), and *DLONG* is set to give a desired ground track spacing of 5.6 km. For this case, the daily flux variations shown previously in Figure 5 were used. The value of *RG* was set to 0.001, and *DG* was computed from the daily flux, assuming a 1-day delay. The ground track repeat cycle for this run was 78 orbits; that is, the time between two adjacent ground track swaths is 78 orbit periods. With all perturbations included, the ground track error varies over a range of about 0.8 km and is fairly well behaved.

Figure 11 shows the number of node crossings as a function of ground track spacing for this run. The longitudes at each crossing are sorted in ascending order, the

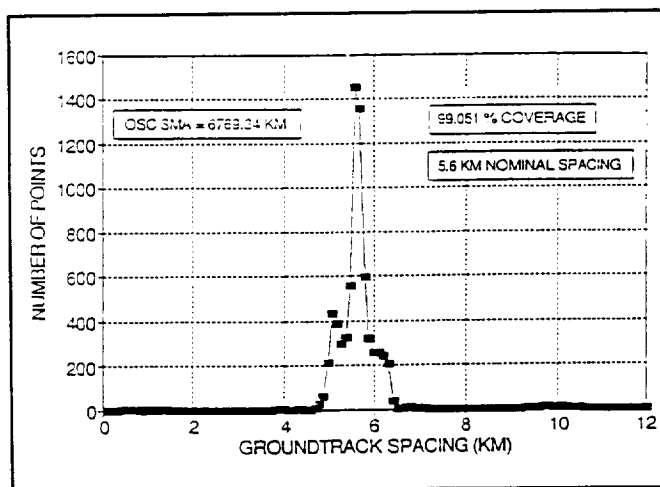


Figure 11. TMLA Ground Track Spacing Daily Flux Variations (1-Day Delay)

difference between two adjacent equator crossings is computed, and the result is assigned to the appropriate 0.1-km-wide bin. This process is repeated until spacing has been computed for all 7157 longitudes (the minimum number for 5.6 km spacing). The number of points in each bin are then plotted.

Ideally, all points would fall in one bin (between 5.5 and 5.6 km or 5.6 and 5.7) to obtain 100 percent coverage and the plot would show one central spike. Perturbations cause errors in the spacing, thus leaving gaps and lowering the overall coverage. The resulting coverage for this run was 99.051 percent, meaning that 380 km total remain uncovered along the equator after one coverage cycle.

Comparison of Results from Different Runs. The results of a series of runs were presented in Table 5. These results include runs at several altitudes, 5.8 and 5.6 km spacing, different flux levels, and constant or varying gains. The table gives a reference run number, spacing, *DLONG*, altitude, gains, orbital elements, solar flux, total delta-V, and resultant coverage. The runs showing "COMP" for the gain (computed by the program) and "DAILY1" for the flux (daily flux with one day delay) represent the most realistic simulations. Other runs with predicted flux and constant gains are included for comparison. Run 8 is the one that was discussed in the previous section.

Also included is a column indicating whether a frozen orbit was used for the run. Several runs were made to determine whether a frozen orbit would yield improved coverage over an arbitrary initial orbit. For a frozen orbit, the heights above the equator at each nodal crossing should show only slight variations over time, which may lead to better control of coverage at the equator. Comparing the runs in Table 5 indicates a small improvement in coverage with the frozen orbit. More details on the frozen orbit will be given in the next section.

Table 5 also demonstrates the importance of choosing the correct value for *DLONG*. For example, Runs 8 and 11 were run with identical initial orbital elements but with values for *DLONG* that differ after the third decimal place (0.001 deg). The one case gives 99.051 percent coverage, while the other only 52.173 percent.

Figure 12 shows the resulting distribution of ground track spacing for Run 11 and shows the peak occurring near 2.9 km. This results in a large overlap between adjacent swaths of about 3.2 km on the average (0.2 to 0.4 km is desirable) leading to large gaps in coverage after 7157 nodal crossings. There were 155 coverage gaps averaging 123.6 km each for a total of 19,158 km uncovered along the equator.

Table 5 also includes the total delta-V for each run. This total represents the total delta-V expended during one coverage cycle (3455 orbits for 5.8 km separation or 3578 orbits for 5.6 km) and depends on the altitude and flux level. The flux levels for the Schatten prediction (PL0391) are

Table 5. Comparative Results of GMAS Runs

Run	Space (km)	DLONG (deg)	Alt (km)	Gain	RGain	Elements	Frozen	Flux	Delta-V (m/sec)	Cover (%)
1	5.8	22.8165345	339.9	0.050	0.023	6718.1400 0.00001 96.8134	N	PL0391	83.57	98.229
2	5.8	22.8165345	336.6	0.050	0.023	6718.1495 0.001419 96.8134	Y	PL0391	83.28	99.283
3	5.8	23.0762551	391.0	0.025	0.001	6769.2400 0.000001 97.0116	N	PL0391	39.42	99.032
4	5.8	23.0762551	387.7	0.025	0.001	6769.2493 0.001398 97.0116	Y	PL0391	37.55	99.653
5	5.8	23.0762551	391.0	COMP	0.001	6769.2400 0.00001 97.0116	N	DAILY1	21.73	98.776
6	5.6	23.0775680	391.1	0.025	0.001	6769.3400 0.00001 97.0116	N	PL0391	40.76	99.115
7	5.6	23.0775680	387.8	0.025	0.001	6769.3400 0.001398 97.0116	Y	PL0391	40.59	99.590
8	5.6	23.0775680	391.1	COMP	0.001	6769.3400 0.00001 97.0116	N	DAILY1	23.78	99.051
9	5.6	23.0775680	387.8	COMP	0.001	6769.3400 0.001398 97.0116	Y	DAILY1	23.65	99.610
10	5.6	23.0766006	391.1	0.025	0.001	6769.3400 0.00001 97.0116	N	PL0391	40.75	52.234
11	5.6	23.0766006	391.1	COMP	0.001	6979.3400 0.00001 97.0116	N	PL0391	40.72	52.173
12	5.6	23.0772455	391.1	COMP	0.001	6769.3400 0.00001 97.0116	N	PL0391	40.71	50.987

Notes:

- Space = Ground track spacing (km)
- DLONG = Longitude difference between successive crossings (deg)
- Alt = Initial altitude at ascending node (km)
- Gain = Displacement gain (COMP = computed by program)
- RGain = Rate gain
- Elements = Osculating orbital elements (semimajor axis, eccentricity, inclination)
- Frozen = Frozen orbit (Yes/No)
- Flux = Solar flux used: PL0391 = Schatten + 2 sigma prediction from March 1991
DAILY1 = Daily varying flux with 1-day delay
- Delta-V = Total delta-V (m/sec) expended during one coverage cycle
- Cover = Percent coverage at equator

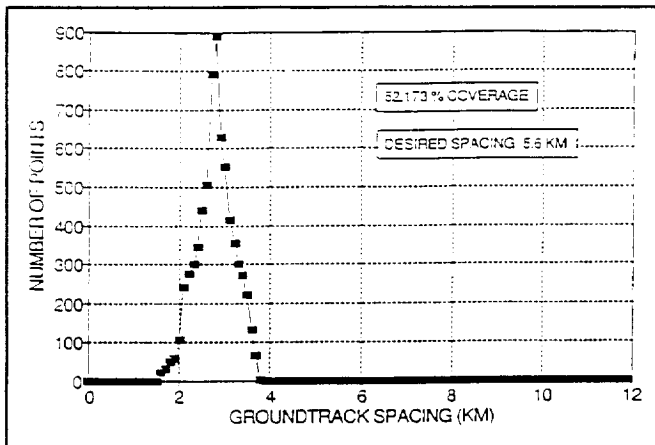


Figure 12. TMLA Ground Track Spacing Initial OSC (SMA = 6769.34)

generally higher than those used for the daily flux runs (DAILY1) and, therefore, show higher delta-Vs. The delta-V will change if the spacecraft mass and area are altered from the values used in this study.

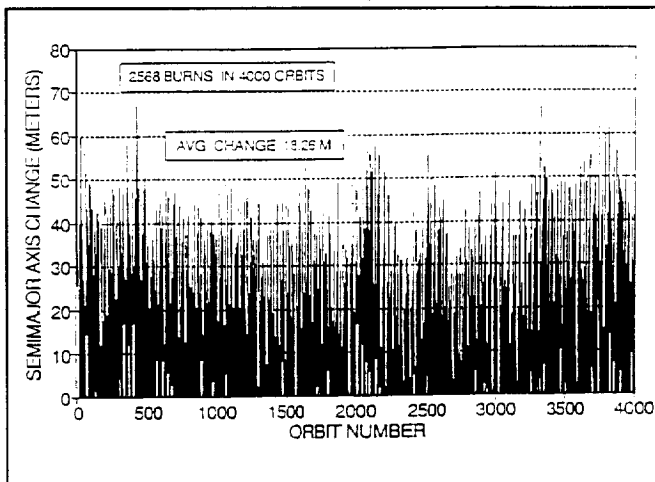


Figure 13. TMLA Delta SMA Per Maneuver Initial OSC (SMA = 6769.34 km)

The expected fuel use during one cycle can be computed from the rocket equation and is given in Table 6 for each run assuming specific impulses of 250 and 600 sec. Also given is the percentage of orbits on which maneuvers occurred (100 percent means a maneuver is performed on every orbit). Figure 13 presents a sample maneuver profile using data from Run 8, showing the semimajor axis change at each maneuver. This case required 2568 maneuvers (two-burn Hohmann transfers) in 4000 orbits; that is, maneuvers were performed at 64.2 percent of the nodal crossings. The changes in semimajor axis ranged from 1 to 79 m with an average change of 18.26 m.

Table 6. Summary of Delta-V and Fuel Requirements

Run	Delta-V (m/sec)	Fuel Required (kg)		Percent of Orbits With Maneuvers
		250 I_{sp}	600 I_{sp}	
1	83.57	7.71	3.24	68.3
2	83.28	7.68	3.23	67.5
3	39.42	3.67	1.54	77.7
4	37.55	3.50	1.46	75.6
5	21.73	2.03	0.85	61.6
6	40.76	3.79	1.59	78.0
7	40.59	3.78	1.58	78.0
8	23.78	2.22	0.93	64.2
9	23.65	2.21	0.92	63.8
10	40.75	3.79	1.59	77.8
11	40.72	3.79	1.59	74.6
12	40.71	3.79	1.58	76.5

Frozen Orbit

As mentioned previously, the use of a frozen orbit was examined to determine whether any benefits existed for TMLA. The concept of a frozen orbit is detailed in Reference 3. In a frozen orbit, the argument of perigee remains in the vicinity of 90 deg (the north point of the orbit), and the altitude above a given latitude remains nearly constant,

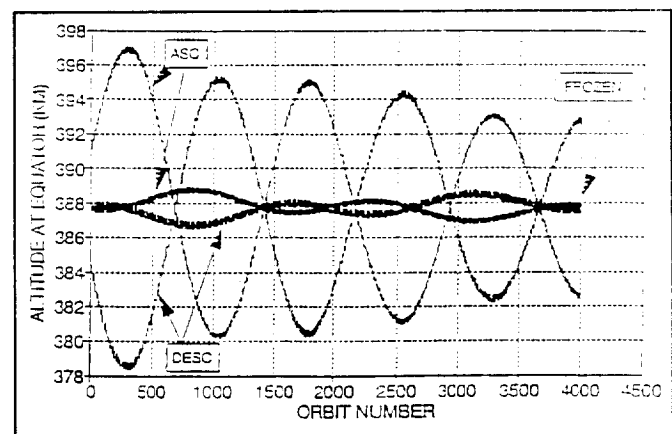


Figure 14. TMLA Height at Nodes (Mean SMA = 6759.62 km) Frozen and Nonfrozen Orbits

assuming maneuvers are performed to counteract the effects of atmospheric drag. This has advantages for an Earth-

observing spacecraft with a repeating ground track, in that each time the spacecraft passes over a given landmark, it will be at nearly the same altitude. This point is illustrated in Figure 14, which shows altitudes above the ascending and descending nodes for frozen and nonfrozen orbits with the same mean semimajor axis. The data were generated by Runs 3 and 4 (see Table 5).

The initial altitudes at the ascending and descending nodes are 391.03 and 384.46 km, respectively, for the nonfrozen orbit. As the orbit evolves in time, the differences between ascending and descending nodal heights increase until the heights differ by almost 19 km. The height differences then decrease to zero and the cycle repeats. The amplitudes of successive cycles, however, decrease with time, which is due to the maneuvers done at the nodal crossings to maintain the orbit. The orbit is slowly evolving to the frozen condition as a result of the maneuvers but may take several ground track cycles to reach that point. The frozen orbit starts with both ascending and descending node altitudes at 387.7 km. As this orbit evolves, the differences in height at the nodes never exceeds about 2.5 km.

The results of the analysis of a small number of cases indicate that the frozen orbit improves the total ground track coverage slightly and greatly improves altitude control over a given part of the orbit. Controlling the altitude in this manner may have advantages for operating the laser or processing laser data.

6. CONCLUSIONS

This paper described an algorithm for a simple autonomous ground track controller for the TMLA mission, using orbit determined from GPS data and a fixed-reference ground track spacing at the equator. Analysis of computer simulations using the control algorithm, with all orbit perturbations including daily solar flux variations, resulted in the following conclusions:

- More than 99 percent coverage at the Equator is obtainable in one cycle of Earth coverage (220 to 230 days) with a 6-km sensor swath width and 5.6 or 5.8 km ground track spacings, in a range of orbit altitudes between 340 and 390 km. A high probability exists that 100 percent coverage will be obtained in a 3-year TMLA mission.
- The percent coverage is critically dependent on the combination of nominal altitude and delta longitude between ascending nodes selected for the mission. A difference of 0.001 degrees in delta longitude, with the same nominal altitude, can make a 47 percent difference in the coverage.
- An orbit that is initially frozen offers a slight improvement in total coverage, compared with an arbitrary near-circular initial orbit. The maintenance maneuvers generated by the algorithm preserve a frozen orbit. A

near-circular orbit becomes a frozen orbit after the passage of time.

REFERENCES

1. Wertz, et al., *Spacecraft Attitude Determination and Control*, D. Reidel Publishing Company, 1978
2. K. Schatten, *Predicted Solar Data as of March 1991*, Goddard Space Flight Center, Code 914, March 1991
3. K. Nickerson et al., "Application of Altitude Control Techniques for Low Altitude Earth Satellites," paper presented at AAS/AIAA Astrodynamics Conference, Jackson Lake, Wyoming, September 1977

FLIGHT MECHANICS/ESTIMATION THEORY SYMPOSIUM

MAY 5-7, 1992

SESSION 3

